IMECE2004-61754

NEUTRON RESIDUAL STRESS MEASUREMENTS ON RAIL SECTIONS FOR DIFFERENT PRODUCTION CONDITIONS

Vladimir Luzin
National Institute of Standards and Technology,
State University of New York, Stony Brook

Jeffrey E. Gordon
Volpe National Transportation Systems Center
Cambridge, MA

Thomas Gnaupel-Herold
NIST Center for Neutron Research
and
University of Maryland, College Park, MD

Henry J. Prask
NIST Center for Neutron Research
National Institute of Standards and Technology
Gaithersburg, MD

ABSTRACT

Rail sectioning with subsequent neutron diffraction experiments has been used to assess residual stresses in the rails. In this study we present the results of neutron stress measurements performed at the NIST Center for Neutron Research (NCNR) on rail sections from rails that were produced under various conditions. Specifically, these are air-cooled, air-cooled and roller-straightened, head-hardened and head-hardened and roller-straightened. More significantly, a head-hardened and roller-straightened rail was also studied after service to elucidate evolution of the service-induced residual stresses. In the latter case both a transverse-cut slice and the central region of a 0.53 m long piece were studied. Measurements on this piece are the first in which triaxial stresses have been determined for an intact rail.

Neutron strain measurements with $3 \times 3 \times 3$ mm^3 spatial resolution were successfully employed for transversally cut slices to verify the difference in the stress state depending on the production process. Although examination of slices allows determination of only two-dimensional stresses in the plane of the slice, additional measurements on obliquely-cut slices, which were also carried out, and utilization of FEM gives the possibility of reconstructing the full triaxial stress distribution. Together, these approaches provide a better understanding of rail fabrication and the possibility of improving the durability and safety of rails in the future.

INTRODUCTION

Rail integrity and prevention of rail failure are the highest priorities for public transportation and the railroad industry. The current understanding of the rail failure problem regards stresses (local contact stress in a vicinity of the wheel/rail contact area and residual stress) as a major factor of the development of the different types of the rail flaws and defects

[1-3]. Other factors such as temperature gradients, gradients in microstructure, wear, and fatigue phenomena seem to be inextricably intertwined with residual stress evolution during rail service. If not origination, at least defect growth is definitely related to this stress evolution.

Failures that happen in the railhead contribute the most to the overall statistics of railroad failures, although broken bases and joint bar defects take place too. The following are examples of the types of railhead failures in which residual stresses can be a driving force:

- Horizontal rolling contact fatigue cracks (subsurface defects which grow parallel to the rail top surface, they cause rail damage when turning toward surface);
- Detail fracture and compound/transverse fissures (transverse defects originate from internal horizontal cracks called shells or surface cracks called head checks)
- Vertically split head

Experimental data and models show the crucial role of stresses in the development of the listed defects [1-3].

Residual stress evolution starts not only after putting a rail into service (service-induced residual stress) but also from the very early stages of rail manufacturing (production-induced residual stress). For example, the head-hardening process not only creates rails with superior hardness properties but also, as a byproduct, it can create residual stresses inherently related to heat treatment of a rail. During roller-straightening rails undergo a number of deformation steps passing through the sequence of rollers what can also create residual stresses.

As a response for the needs in rail integrity and safety DOT started the Track System Research Program with research conducted by the Volpe National Transportation Center and sponsored by the Federal Railroad Administration. Specifically, the Volpe Center is involved in engineering studies to

determine the effects of rail production conditions and grinding strategy on the distribution and magnitude of production-induced and service-induced residual stresses [3,4].

Recent experimental work [4], including neutron diffraction stress measurements that have been done using the BT8 diffractometer at the NIST Center for Neutron Research, is a part of these collective efforts.

Table 1. Rails samples specification.

Sample	Production conditions	Form
#1	Air-cooled only, no service	T&O slices
#2	Air-cooled and roller-straightened, no service	T&O slices
#3	Head-hardened only, no service	T&O slices
#4	Head-hardened and roller-straightened, no service	T&O slices
#5	After revenue service	T&O slices + 0.5m piece
T = transverse; O = 45°oblique		

The measurement of stress by means of neutron diffraction has several advantages over other methods. Thermal neutrons (with wavelength on the order of 1 Å) have relatively high penetration with respect to x-rays. For example, in steel the half-value thickness (or the thickness of half-attenuation) for a thermal neutron beam is approximately 6 mm (3 µm for x-rays) while aluminum is even more transparent with a half-value thickness around 70 mm (50 µm for x-rays). Due to this high penetration, subsurface measurements are possible with neutrons. Moreover, this allows determination of the whole strain tensor (planar in x-ray experiments or using strain gauge techniques) nondestructively, compared with destructive relaxation methods that involve cutting and drilling. Among nondestructive techniques only synchrotron radiation can be competitive with neutron diffraction [5,6].

In the last decade significant progress has been achieved in the application of neutron diffraction to stress determination in rails [7-10]. Usually, rather thin slices of the order of 10 mm are used for this kind of measurement. The drawback of this slicing technique is that the stress component in the direction perpendicular to the slice plane is lost because of stress relaxation. Although one would like to obtain complete stress tensor data from measurements on an intact (or long piece of) rail, experimental realization of such an experiment has not been achieved because of the long path length required. One can estimate that for a neutron flight path of 75 mm, in the worst case for the rail measured in 90°-geometry, beam intensity is reduced by factor of 10000. At a fixed gauge volume increasing measurement time or special attempts to raise beam intensity are the only means of compensation.

This was achieved at the NCNR BT-8 diffractometer [4] by incorporating a focusing Si-monochromator and a position sensitive detector. In addition, great care was taken to minimize the path length for each individual measurement of each strain component.
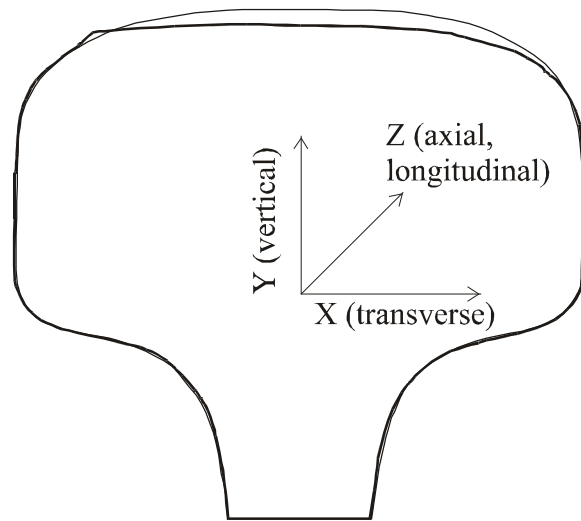

Fig. 1. Worn rail profile of the series #5 and unworn profile of series #1-4.

SAMPLES

All rails used in the investigation were commercially produced by RMSM (Rocky Mountain Steel Mills) with the specification 132RE. Steps in the production line include a deep head-hardening process and roller-straightening to achieve a hardness of the rail as high as approximately 400 Brinell, which is an excellent long-term wear protection. Samples that were furnished to NIST for stress measurement are listed in Table 1.

All samples were first saw-cut from rails as slices approximately 12 mm thick, which were subsequently cut again by EDM (Electric Discharge Machining) to 6 mm thickness to minimize absorption of the beam in the neutron experiment.

Sample series #5, in addition to transverse and oblique slices, includes a long rail section, approximately 530 mm in length. It was provided by the High Tonnage Loop facility at the Transportation Technology Center after subjecting it to 39-ton axle load service. This piece of rail was cut from a defect-free area adjacent to a detected transverse defect so that the rail stress condition is very close to the condition of the area where the defect occurred. The piece was chosen long enough to preserve stresses intact and, according to FEM calculations [11], with negligible end effects at the center of the rail.

Series #5 exhibits a typical worn profile. For the purpose of comparison, the worn and unworn series profiles are shown in Fig. 1. These profiles were obtained by an optical scan with subsequent digitizing.

NEUTRON STRESS EXPERIMENT

Slices.

As was mentioned above neutron stress measurements have proved to be successful in measurements of rail slices. Measurements of the rail slice are less challenging. A standard set of data comprises measurements at 366 locations (mesh points) in the rail head in four different directions for each point in the 3x3 mm experimental mesh (Fig. 2). With a nominal gauge volume of 3x3x3 mm³ one individual measurement took
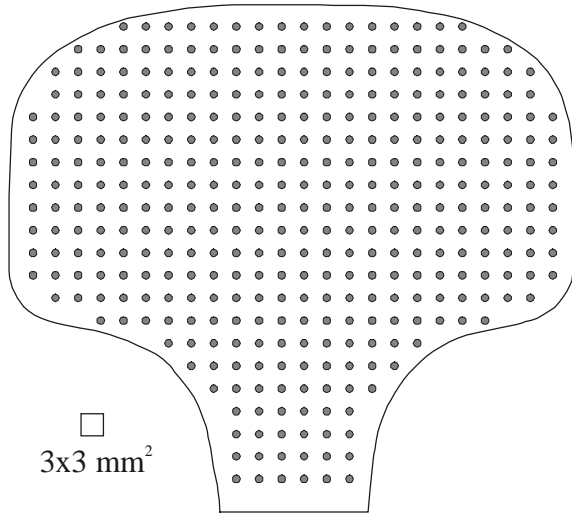
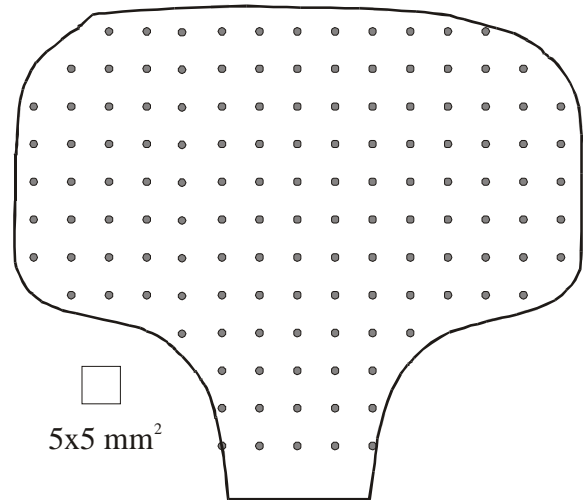**Fig. 2.** Experimental 3x3 mm mesh used for slice mapping.

Fig. 3. Experimental 5x5 mm mesh used for long piece mapping.

2 min using the (211) reflection at the scattering angle of $2\vartheta=90.4°$, wavelength $\lambda=1.67\text{Å}$.

Long rail piece

As described above neutron stress measurements on the long piece of rail is a challenging task primarily because of very high attenuation when it is needed to penetrate through the bulk of material. In these circumstances the selection of the experimental conditions is critical. These experimental conditions include:

- scattering geometry (defines gauge volume shape, instrument resolution and neutron flight-path in the material)
- gauge volume size (defines diffraction peak intensity and experimental mesh)
- sample orientation (chosen to minimize neutron flight path through material)
- choice of the diffraction reflection

Optimization of all these parameters allowed us to achieve the desired accuracy of $\Delta d/d = 5 \times 10^{-5}$. Specifically, the iron (211) reflection was chosen with a nominal beam cross section of 5x5 mm^2. A 5x5x5 mm^3 gauge volume was used for the axial component and a 5x5x20 mm^3 gauge volume for the vertical, transverse and shear components. Accordingly, a 5x5 mm mesh was used for each component measured. While the vertical, transverse and shear components could be measured at almost 90°-scattering geometry, the axial component was more difficult to measure and a 60°-scattering geometry was chosen to optimize scattering conditions. In order to maintain the required accuracy the measurement time for each mesh point was chosen according to the depth of the gauge volume inside the material. For the quantitative evaluation of the measurement time, maps for the neutron flight-path inside of material were created for each particular experiment geometry. The measurement time varied from 5 seconds to 8 hours depending on path length and gauge volume.

DATA ANALYSIS

Slices

The neutron diffraction patterns collected using a position sensitive detector were fitted by Gaussian peak profiles. This fitting procedures results in a set of d-values, each of which is associated with a location (x,y,z) in the sample and with the direction (ψ,φ) in which it was measured. In order to get elastic strain values, $\varepsilon=(d-d_0)/d_0$, from d-values the d_0-value of the unstressed material must be known. After that the main equation of the diffraction stress analysis can be applied to recalculate stress from the experimentally determined stresses,

$$\sigma_{ij} = \frac{1}{\frac{1}{2}S_2(hkl)}\left\{\varepsilon_{ij} - \delta_{ij}\frac{S_1(hkl)}{\frac{1}{2}S_2(hkl)+3S_1(hkl)}(\varepsilon_{11}+\varepsilon_{22}+\varepsilon_{33})\right\}.$$

For the (211) reflection of steel $S_1(211)=-1.3\times10^{-6}MPa^{-1}$ and $\frac{1}{2}S_2(211)=5.83\times10^{-6}MPa^{-1}$. This equation can also be used for evaluation of the d_0-value from the assumption that the axial stress component is zero, $\sigma_{33}=0$, because of stress relaxation. Mathematically, measurement of four strain components in four directions, ε_{11}, ε_{22}, ε_{33} and ε_{12}, allow us to recalculate four unknowns as σ_{11}, σ_{22}, σ_{12} and d_0 under the condition $\sigma_{33}=0$. This requirement can be applied pointwise but for better statistical accuracy it can be averaged over the whole cross section. As a result, it yields the average σ_{33}-component equal to zero with local statistical deviations (see experimental result below). For the sample series #1-4 (unused rails) one unique d_0-value for each rail type was used while in series #5 we observed a gradient of the d_0-value in the railhead section.

An error analysis based on counting statistics has been done using standard error propagation techniques resulting in typical stress value errors of ±15 MPa for all components.

Long rail piece

A similar data analysis was done on the long rail piece with only a few distinctions. All four stress components, σ_{11}, σ_{22}, σ_{33}

and σ_{12}, must be defined from four measured strain components ε_{11}, ε_{22}, ε_{33} and ε_{12}. In this case separate measurements were performed to obtain the d_0-value of the unstressed material to make use of the formula $\varepsilon=(d-d_0)/d_0$. Five cubic coupons, 7 mm on a side, were cut by EDM (electric discharge machining) from five different locations of the same rail for the d_0 measurements (three in the railhead, one in the web and one in the foot). This procedure utilizes the fact that macroscopic
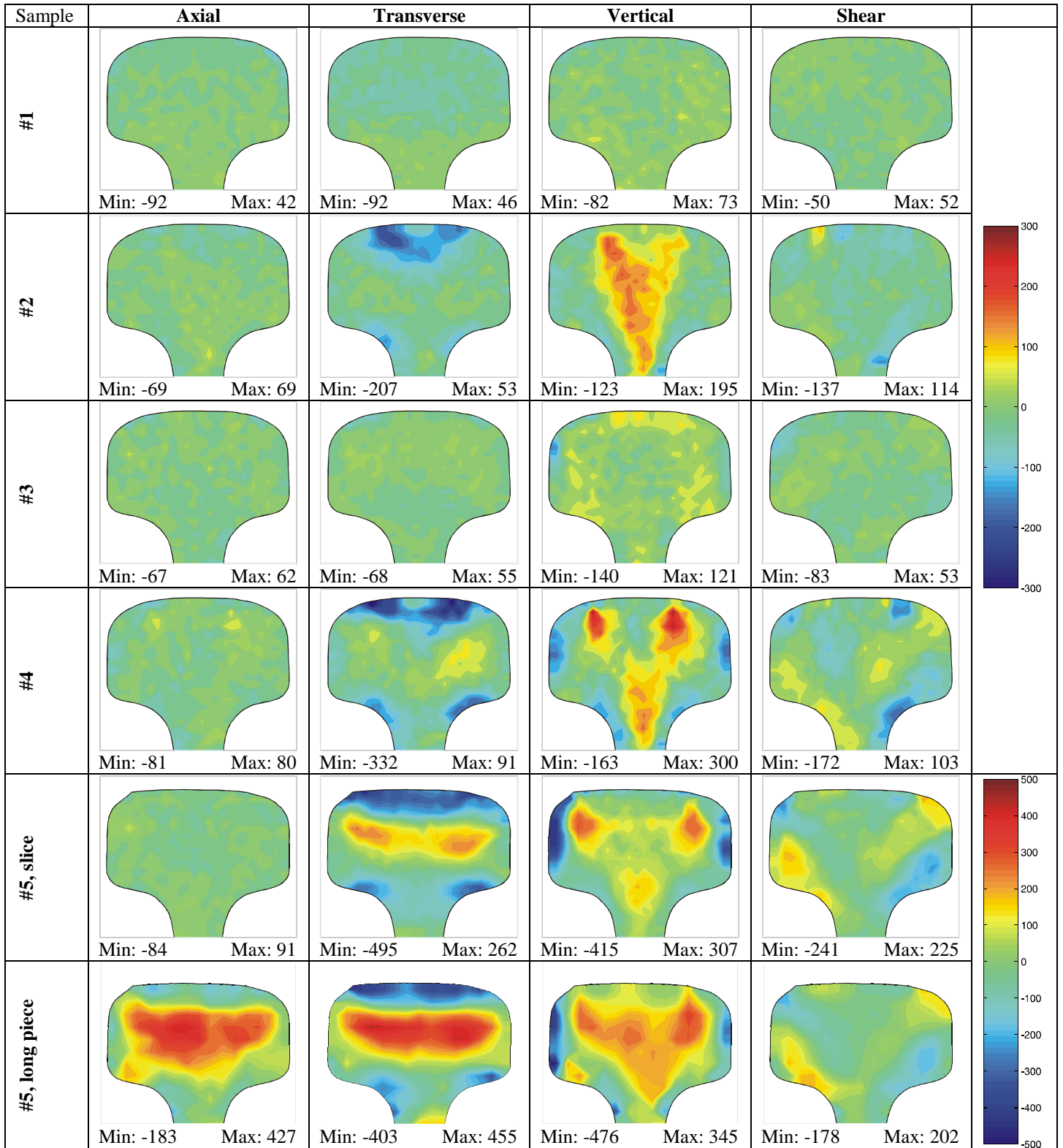

Fig. 4. Maps of stress tensor component distributions for the slices (#1-5) and the long rail piece (#5).

Sample	Axial	Transverse	Vertical	Shear
#1	Min: -92 Max: 42	Min: -92 Max: 46	Min: -82 Max: 73	Min: -50 Max: 52
#2	Min: -69 Max: 69	Min: -207 Max: 53	Min: -123 Max: 195	Min: -137 Max: 114
#3	Min: -67 Max: 62	Min: -68 Max: 55	Min: -140 Max: 121	Min: -83 Max: 53
#4	Min: -81 Max: 80	Min: -332 Max: 91	Min: -163 Max: 300	Min: -172 Max: 103
#5, slice	Min: -84 Max: 91	Min: -495 Max: 262	Min: -415 Max: 307	Min: -241 Max: 225
#5, long piece	Min: -183 Max: 427	Min: -403 Max: 455	Min: -476 Max: 345	Min: -178 Max: 202

residual stresses are relaxed in the small coupons. With the d_0-value known the sequence of strain and stress calculations can be completed.

A counting statistics based error analysis for this sample gives typical stress value uncertainty (standard deviation) of ±15 MPa for transverse and vertical components and ±25 MPa for the axial component.

RESULTS
Results in the form of 2D maps are shown in Fig. 4 for all slice samples and one long piece. Four components of the stress tensor are plotted and minimum and maximum values are provided.

DISCUSSION

Slices
The influence of the rail production condition on the residual stresses in the railhead was examined. Two-dimensional distributions of stresses were determined in slices by means of neutron diffraction. Our results evoke the following conclusions

- Simple air-cooling (#1) does not produce any residual stresses; small variations in stress maps for this sample are of a statistical nature.
- Roller-straightening (#2) induces moderate stresses (compressive zone of transverse stress just under the running surface while the center core is under vertical tension).
- Head-hardening (#3,4), while having great impact on hardness, has a less pronounced effect on residual stresses. Head-hardening sample (#3) differs only slightly from the air-cooled only sample (#1). Head-hardening also produces only little redistribution in stress how it follows from the comparison of the head-hardening, roller-straightened sample (#4) with the roller-straightened one (#2).
- Rail service is a major factor for residual stress development in rails especially in the near-surface area in which significant vertical compression appears (#5).

Long rail piece
The main result of the neutron measurements is that for the first time a 3D stress map of the stresses in a long piece of intact rail was determined nondestructively. An area of tensile stresses in the central core of the rail was found for the axial component. The surrounding area is in moderately compressive stress. However, considering only the railhead area, stress balance for the axial component (in the transverse plane) is not achieved. This is evidence that overall tensile axial stress in the railhead must be balanced in part by compressive stress in the web and foot. Measurements in these regions have not been completed yet. However, early measurements on rail slices [9] and recent results using the contour method [12] indicate that regions of high compression occur in the axial direction in both the web and the foot.

A comparison of the 3D stresses with the 2D stresses in a slice sample from the same rail can be made readily. Transverse, vertical and shear stresses for the long rail piece and the slice are numerically similar but not identical, as one would expect. Qualitatively, the results of the present investigation confirm that major features of the stress distribution in the vertical and transverse directions are reasonably well-preserved when a slice is cut. Quantitative analysis of the maps indicates that some stress redistribution in the slice takes place resulting in the change of, for example, extreme values.

Before drawing definitive conclusions in comparing the long rail piece and slice results it should be noted that a number of factors have not yet been completely included in the analysis:

- There is some evidence [13] that radiation attenuation effects can play a certain role resulting in a peak position shift that would alter the stress results;
- Peak shift effects can occur due to the use of different gauge volumes and meshes (5x5x5 against 3x3x3). This is especially important for the regions of high stress gradients near to the top (contact) surface of the rail.
- So called partial illumination effects can also give rise to substantial variations of experimental results in the points close to the surface.

It should be mentioned that overall stress balance may be shifted somewhat due to the presence of cementite in the hypereutectic alloy.

SUMMARY
Knowledge of the residual stresses in rails is important because it affects rail performance and integrity and eventually has economic impact on the railroad industry. Several measurement techniques, both destructive and nondestructive, were developed to monitor residual stresses. However all these monitoring techniques lack a clear benchmark against which their accuracy, reliability and effectiveness can be judged. Recently developed numerical methods mainly based on finite element analysis also need such experimental data as a reference to ensure their validity. In the present work the first nondestructive determination of the triaxial stress distribution in an intact rail piece is presented. These results can provide such a benchmark due to the extent and detail of the obtained data. This benchmark can only be improved when higher intensity sources are available allowing significant improvements in spatial resolution.

These results also can verify the validity of the slicing technique, which is frequently used in neutron and synchrotron diffraction measurements, and the assumption that in-plane stresses are preserved after slice cutting.

Finally, this investigation explicates the influence of rail production treatments on the formation of the residual stresses during rail fabrication.

REFERENCES
[1] J. Orkisz and M. Holowinski, 1992, *Rail Quality and Maintenance for Modern Railway Operation*, Kluwer Academic Publishers, The Niderlands.

[2] O. Oringer et al., eds., 1992, *Residual Stress in Rails: Effects of Rail Integrity and Railroad Economics, Vol. I: Field Experience and Test Results*, Kluwer Academic Publishers, The Niderlands.

[3] http://www.volpe.dot.gov/sdd/pubs-integrity.html

[4] T. Gnaupel-Herold, P.C. Brand, H.J. Prask, 1999, "Neutron Diffraction Investigation of Risidual Stresses in Transverse/Oblique Rail Slices Subjected to Different Grinding Stratagies", Report NISTIR 6305, U.S. Department of Commerce, Technology Administration.

[5] P.J. Webster, D.J. Hughes, G. Mills and G.B.M Vaughan, 2002, "Synchrotron X-Ray Measurements of Residual Stress in a Worn Railway Rail", Mater. Sci. Forum, **404-407**, pp. 767-772.

[6] D.J. Buttle, N. Collett, P.J. Webster, D.J. Hughes and G. Mills, 2002, "A comparison of MAPS and Synchrotron X-Ray Methods: Stress Measured in Railway Rail Sections", Mater. Sci. Forum Vols, **404-407**, pp. 881-886.

[7] P.J. Webster, K.S. Low, G. Mills, and G.A. Webster, 1990, "Neutron Measurementsof Residual Stresses in a Used Raiway Rail", Mat. Res. Soc Symp. Proc., **166**, pp. 311-316.

[8] G.A. Webster, P.J. Webster, M.A.M. Bourke, K.S. Low, G. Mills, H.J. McGillivray, D.F. Cannon and R.J. Allen, 1992, "Neutron Diffraction Determinations of Residual Stress Patterns in Railway Rails", *Residual Stress in Rails, ibid.,* pp. 143-152.

[9] P.J. Webster, G. Mills, X. Wang and W.P. Kang, 1992, "Residual Stress Measurements in Rails by Neutron Diffraction", *Rail Quality and Maintenance for Modern Railway Operation*, ibid., pp. 307-314.

[10] J.H. Root, T.M. Holden, R.J. Klassen, C. Smallman, B. Maxfield, and N.R. Gore, 1992, "Neutron Diffraction Measurements of Residual Stress in Rails", *Rail Quality and Maintenance for Modern Railway Operation*, ibid., pp. 315-324.

[11] B. Talamini and J.E. Gordon, to be published.

[12] J. Keleher, M.B. Prime, D. Buttle, P.M. Mummery, P.J. Webster, J. Shackleton and P.J. Withers: Proceedings of the MECA-SENS Conf., Manchester, England (2003), in press.

[13] T.C. Hsu, F. Marsiglio, J.H. Root and T.M. Holden, 1995, "Effects of Multiple Scattering and Wavelength-dependent Attenuation on Strain Measurements by Neutron Scattering", J. of Neutron Research, **3(1)**, pp. 27-39.